

## Analysis of Geometric Parameters for Fully Developed Laminar Flow Between Cylinders Arranged in Regular Array

D-R Lee

### 정규배열내의 실린더 사이에서의 완전발달된 층류 유동의 기하학적 계수의 해석

이 동 렬

**Key words** : Power law fluid flow(멱법칙유체유동), Channel flow of noncircular cross section(비원형 도관유동), Longitudinal laminar flow of non-Newtonian fluids(비뉴톤 유체의 축방향 층류유동)

#### Abstract

Considerable interest has evolved in the flow of non-Newtonian fluids in channels of noncircular cross section in compact heat exchangers. Analytical solution was developed for prediction of the flow rate and maximum velocity in steady laminar flow of any incompressible, time-independent non-Newtonian fluids in straight closed and open channels of arbitrary, but axially unchanging cross section. The geometric parameters and function of shear stress describing the behavior of the fluid model were evaluated for fluid flow among a bundle of rods arranged in triangular and square array. Numerical values of dimensionless maximum velocities, mean velocities, pressure-drop-flow parameters and friction factors were evaluated as a function of porosity and pitch-to-radius ratio.

#### 1. INTRODUCTION

The flow of non-Newtonian fluids has been the subject of increasingly extensive study in recent years. Considerable interest has evolved in the flow of non-Newtonian fluids in channels of non-circular cross section. A method has

recently been proposed by Kozicki et al.<sup>[1]</sup> and Kozicki and Tiu<sup>[2]</sup> for prediction of the flow rate and maximum velocity in steady laminar flow of any incompressible, time-independent non-Newtonian fluids in straight closed and open channels of arbitrary, but axially unchanging cross section. The method requires only a

knowledge of two geometry parameters and a function of shear stress characterizing the behavior of the fluid model.

Kozicki and his coworkers<sup>[11],[2],[3],[4],[5]</sup> have presented a general approximate method for calculating laminar pressure drops for non-Newtonian fluids flowing in ducts and open channels. They considered a wide variety of fluid models such as Bingham, and Ellis fluids.

Kozicki et al.<sup>[1]</sup> introduced a new generalized Reynolds number,  $Re^*$  such that the friction factor for fully developed laminar flow of a power law fluid through noncircular duct having a constant cross-sectional area is given by a familiar equation;

$$f = \frac{16}{Re^*} \tag{1}$$

where

$$Re^* = \frac{\rho \bar{u}^{-2-n} d_h^n}{8^{n-1} (b + \frac{a}{n}) \kappa} \tag{2}$$

The geometric parameters  $a$  and  $b$  depend on the geometry of the cross-section. Since data presented in the literature for Newtonian fluids are generally more complete and precise than that available for other fluids, values of  $a$  and  $b$  were calculated from expressions for the bulk velocity and maximum velocity derived mathematically using the Navier-Stokes equation.

The predicted values of the geometric parameters  $a$  and  $b$  are thus in well agreement with the published values for Newtonian fluids<sup>[1]</sup>.

For a circular duct, the values of  $a$  and  $b$  are 0.25 and 0.75, respectively and the generalized Reynolds number becomes tantamount to  $Re_g$ , defined as  $\rho \bar{u}^{-2-n} d_h^n / \kappa$  proposed by Metzner and Reed<sup>[6]</sup>.

$$Re^* = \frac{\rho \bar{u}^{-2-n} d_h^n}{8^{n-1} (0.75 + \frac{0.25}{n}) \kappa} \tag{3}$$

Dividing  $Re_g$  by Eq. (2) and substituting Eq.(1) into (3), the following equation is obtained;

$$f \cdot Re_g = 2^{3n+1} (b + \frac{a}{n}) \tag{4}$$

Values of  $a$  and  $b$  for circular sections were introduced directly by evaluation of the Mooney-Rabinowitsch equation. The analytical solutions available in Bird et al<sup>[7]</sup> for concentric annuli were used to obtain the geometric parameters for this section. For rectangular, elliptical, and isosceles triangular sections, the solutions for Newtonian fluids presented by Lundgren, Sparrow, and Starr<sup>[8]</sup> were utilized in the examinations of the geometric parameters  $a$  and  $b$ .

The purpose of this research is to report the geometric parameters  $a$  and  $b$  evaluated for fluid flow among a bundle of rods arranged in triangular and square array. These will be evaluated on the base of analytic solutions for longitudinal laminar flow of Newtonian fluid between cylinders arranged in regular array<sup>[9],[10],[11]</sup>. Numerical results of dimensionless maximum velocities, mean velocities, pressure-drop-flow parameter and friction factors will be evaluated as a function of porosity and pitch-to-radius ratio  $s/r_0$ . Finally, the maximum velocities and mean velocities will be used to calculate the geometric parameters  $a$  and  $b$ .

## 2. LONGITUDINAL LAMINAR FLOW BETWEEN CYLINDERS ARRANGED IN REGULAR ARRAY FOR NEWTONIAN FLUIDS

### 2.1 Mathematical Analysis

The geometry considered in the present analysis is shown in Fig. 1. From the symmetry of the situation it is easily seen that attention need be focused on only the cross-hatched element. The enlarged view is shown at Fig. 2.

The conservation principle requires that under steady state condition the net change of momentum must be equal to the forces. For fully developed flow of Newtonian fluids, the governing equation is so obtained in cylindrical coordinate system

$$\frac{\partial^2 u}{\partial r^2} + \frac{1}{r} \frac{\partial u}{\partial r} + \frac{1}{r^2} \frac{\partial^2 u}{\partial \theta^2} = \frac{1}{\mu} \frac{dp}{dx} \tag{5}$$

Eq. (1) is frequently called Poisson's equation and the general solution is<sup>(12)(13)(14)(15)(16)(17)</sup>

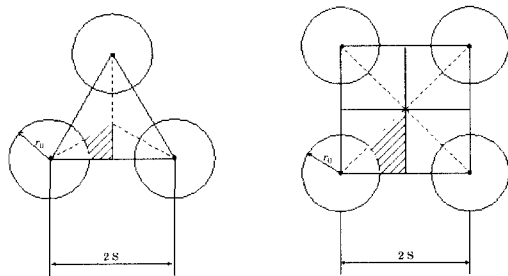


Fig. 1 Geometry of channels arranged in regular array

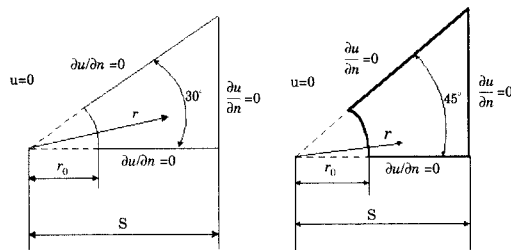


Fig. 2 Cross-hatched element of channel

$$u = A + B \cdot \ln r - \frac{r^2}{4} \left( -\frac{1}{\mu} \frac{dp}{dx} \right) + \sum_{K=1}^{\infty} (C_K r^K + D_K r^{-K}) \cdot (E_K \cos K\theta + F_K \sin K\theta) \tag{6}$$

The boundary conditions to determine the constants in Eq. (6) are expressed as follows;

#### 2.1.1 For the case of triangular array

$$\text{at } \theta = 0, \frac{\partial u}{\partial n} = \frac{\partial u}{\partial \theta} = 0, F_K = 0 \tag{7}$$

$$\text{at } \theta = \frac{\pi}{6}, \frac{\partial u}{\partial n} = \frac{\partial u}{\partial \theta} = 0, K=6, 12, 18, \dots \tag{8}$$

$$\text{at } r = r_0, u=0, A = -B \ln r_0 + \frac{r_0^2}{4} \left( -\frac{1}{\mu} \frac{dp}{dx} \right) \tag{9}$$

$$D_K = -C_K r_0^{2K}$$

Also, for overall force balance

$$\int_0^{\pi/6} \int_{r_0}^{s/\cos\theta} \left( \frac{dp}{dx} \right) r dr d\theta = \int_0^{\pi/6} \mu \left( \frac{\partial u}{\partial r} \right)_{r=r_0} r_0 d\theta \tag{10}$$

The evaluation of this equation from Eq. (10) yields

$$B = \frac{\sqrt{3}}{\pi} s^2 \left( -\frac{1}{\mu} \frac{dp}{dx} \right) \tag{11}$$

Bring together the findings of the previous paragraph, Eq. (6) becomes

$$u = \frac{\sqrt{3}}{\pi} s^2 \left( -\frac{1}{\mu} \frac{dp}{dx} \right) \ln \frac{r}{r_0} - \frac{1}{4} \left( -\frac{1}{\mu} \frac{dp}{dx} \right) (r^2 - r_0^2) + \sum_{j=1}^{\infty} G_j \left( r^{6j} - \frac{r_0^{6j}}{r^{6j}} \right)^{12j} \cos 6j\theta$$

$$\text{where } G_j = C_j E_j \tag{12}$$

Finally, the boundary condition of  $\frac{\partial u}{\partial n} = 0$  at  $r = \frac{s}{\cos\theta}$  being imposed on Eq. (12), one finds after rearrangement

$$\sum_{j=1}^{\infty} \Delta_j (\cos\theta)^{1-6j} \left[ \cos(6j-1)\theta + \left( \frac{r_0 \cos\theta}{s} \right)^{12j} \cos(6j+1)\theta \right] + \frac{\sqrt{3}}{\pi} \cos^2\theta - \frac{1}{2} = 0 \tag{13}$$

where

**Table 1. Numerical Values of  $\Delta_j$**

| $\frac{S}{r_0}$ | $\Delta_1$ | $\Delta_2$ | $\Delta_3$ | $\Delta_4$ | $\Delta_5$ |
|-----------------|------------|------------|------------|------------|------------|
| 4.00            | -0.0505    | -0.0008    | 0.0000     |            |            |
| 2.00            | -0.0505    | -0.0008    | 0.0000     |            |            |
| 1.50            | -0.0502    | -0.0007    | 0.0000     |            |            |
| 1.20            | -0.0406    | 0.0007     | 0.0002     | 0.0000     |            |
| 1.10            | -0.0416    | 0.0028     | 0.0004     | 0.0000     |            |
| 1.05            | -0.0368    | 0.0043     | 0.0003     | -0.0001    | 0.0000     |
| 1.04            | -0.0357    | 0.0046     | 0.0002     | -0.0001    | 0.0000     |
| 1.03            | -0.0345    | 0.0049     | 0.0002     | -0.0001    | 0.0000     |
| 1.02            | -0.0332    | 0.0051     | 0.0000     | -0.0001    | 0.0000     |
| 1.01            | -0.0319    | 0.0052     | -0.0001    | -0.0002    | 0.0000     |
| 1.00            | -0.0305    | 0.0053     | -0.0003    | -0.0002    | 0.0000     |

$$\Delta_j = G_j \frac{6j S^{6j}}{\left(-\frac{1}{\mu} \frac{dp}{dx}\right) S^2}$$

Eq. (13) provides a method for determining the  $\Delta_j$  (that is  $G_j$ ). Lundgren et al.<sup>[8]</sup> applied Eq.(13) at 6 points along the boundary. They successively evaluated Eq. (8) at six values of  $\theta$  between  $0^\circ$  and  $30^\circ$ . This provided six equations. They truncated the series after six terms (that is  $l=6$ ) so that there are sufficient simultaneous equations to evaluate the coefficients  $\Delta_1, \Delta_2, \Delta_3, \dots, \Delta_6$ . This procedure was repeated with the use of seven boundary points and seven series coefficients, and so forth. The sets of coefficients  $\Delta_j$  from these repeated calculations were compared. It was immediately seen that adding additional terms to the series did not significantly affect the numerical values of the first few coefficients. Further it was found that only these first coefficients are important in the computation of shear stress and velocity distribution.

Numerical values of  $\Delta_j$  computed as outlined above, are listed in Table 1. With the determination of the  $\Delta_j$  (that is  $G_j$ ) one may return to Eq. (12) and state that the velocity distribution for the triangular array is now available.

**Table 2. Numerical Values of  $\delta_j$**

| $\frac{S}{r_0}$ | $\delta_1$ | $\delta_2$ | $\delta_3$ | $\delta_4$ | $\delta_5$ | $\delta_6$ |
|-----------------|------------|------------|------------|------------|------------|------------|
| 4.00            | -0.1253    | -0.0106    | -0.0006    | 0.0000     |            |            |
| 2.00            | -0.1250    | -0.0105    | -0.0006    | 0.0000     |            |            |
| 1.50            | -0.1225    | -0.0091    | -0.0002    | 0.0000     |            |            |
| 1.20            | -0.1104    | -0.0024    | -0.0015    | 0.0003     | 0.0001     | 0.0000     |
| 1.10            | -0.0987    | -0.0036    | 0.0029     | 0.0005     | 0.0000     |            |
| 1.05            | -0.0904    | -0.0073    | 0.0032     | 0.0002     | -0.0001    | 0.0000     |

**2.1.2 For the case of square array**

By a similar method the velocity distribution for the square array is obtained

$$u = \frac{2}{\pi} S^2 \left(-\frac{1}{\mu} \frac{dp}{dx}\right) \ln \frac{r}{r_0} - \frac{1}{4} \left(-\frac{1}{\mu} \frac{dp}{dx}\right) (r^2 - r_0^2) + \sum_{j=1}^{\infty} G_j \left(r^{4j} - \frac{r_0^{8j}}{r^{4j}}\right) \cos 4j\theta \tag{14}$$

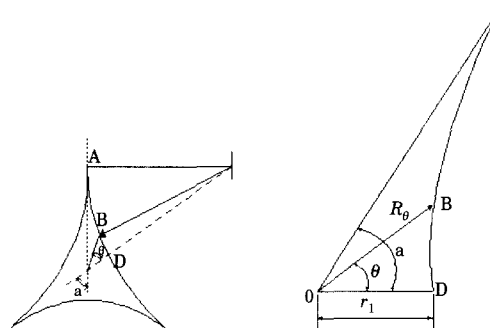
where 
$$\delta_j = G_j \frac{4j S^{4j}}{\left(-\frac{1}{\mu} \frac{dp}{dx}\right) S^2}$$

and numerical values of  $\delta_j$  are listed in Table 2.

**2.1.3 For the case of cylinders touching**

Shih<sup>[9]</sup> provided solutions to laminar flow in three-point-star and four-point-star conduits, which is the limit case of cylinders touching.

The coordinate axis is placed at O, in Fig. 3. The starting equation is again Poisson's equation



**Fig. 3 Geometry of three-point-star and four-point-star conduits**

$$\frac{\partial^2 u}{\partial r^2} + \frac{1}{r} \frac{\partial u}{\partial r} + \frac{1}{r^2} \frac{\partial^2 u}{\partial \theta^2} = q \tag{15}$$

where  $q = \frac{1}{\mu} \frac{dp}{dx}$

The general solution is

$$u(r, \theta) = A + B \ln r - \frac{r^2}{4} q + \sum (C_K r^K + D_K r^{-K}) (E_K \cos K\theta + F_K \sin K\theta) \tag{16}$$

at  $r = 0$ ,  $u$  is finite,  $B = 0$

$$D_K = 0$$

at  $\theta = 0$ ,  $\frac{\partial u}{\partial \theta} = 0$ ,  $F_K = 0$

at  $\theta = \theta_0$ ,  $\frac{\partial u}{\partial \theta} = 0$ ,  $K = \frac{n\pi}{a}$ ,  $n = 1, 2, 3, \dots$

Bring together the information, one gets :

$$u(r, \theta) = A - \frac{q}{4} r^2 + \sum A_K r^K \cos K\theta \tag{17}$$

where  $A_K = C_K E_K$

$$\text{at } (r, \theta) = (r_i, \theta_0), u = 0, A = \frac{q}{4} r_i^2 - \sum A_K r_i^K \tag{18}$$

Substitute Eq. (18) back into Eq. (17), one obtains :

$$u(r, \theta) = \frac{q}{4} [r_i^2 - r^2 - \sum A'_K (r_i^K - r^K \cos K\theta)] \tag{19}$$

where  $A'_K = \frac{4A_K}{q}$

Since boundary curve may be expressed as  $r = f(\theta)$  for  $0 \leq \theta \leq a$  one may formulate as  $u(r_\theta, \theta) = 0$ , for  $0 \leq \theta \leq a$ ; ( $r_\theta = f(\theta)$ ) so Eq. (19) yields

$$r_i^2 - r_\theta^2 = \sum A'_K (r_i^K - r_\theta^K \cos K\theta) \quad 0 < \theta \leq a \tag{20}$$

Eq. (19) is arranged in a dimensionless radial variable,  $R = r/r_1$ ,

$$u(R, \theta) = \frac{qr_i^2}{4} \left[ 1 - R^2 + \sum_{n=1}^N C_n (1 - R^K \cos K\theta) \right] \tag{21}$$

The compound constants ( $A'_K r_i^{K-2}$ ) are replaced by  $C_n$ , which are to be determined by

**Table 3. Function Coefficients for Solution to Flow in Star Conduits of p Points**

| P | C <sub>1</sub> | C <sub>2</sub> | C <sub>3</sub> | C <sub>4</sub> | C <sub>5</sub> | C <sub>6</sub> |
|---|----------------|----------------|----------------|----------------|----------------|----------------|
| 3 | 1.43334        | 1.17184        | 1.10089        | 0.39062        | -0.32975       | -0.25817       |
| 4 | 1.41642        | 1.15781        | 0.40566        | -0.90891       | -1.32956       | -0.54210       |

a set of N equations generated by N boundary points. By discarding the terms after N in the series of Eq. (21) and substituting into it, one pair at a time, the coordinate values of N ( $R_\theta, \theta_i$ ) pairs along the boundary curve at arbitrarily selected N boundary points ( $R_\theta, \theta_i$ ),  $i = 1, 2, \dots, N$ , a set of N linear algebraic equations each containing the first N.  $C_n$  can be easily generated. This set of linear equations can be solved to obtain the N coefficients needed in the series solution given by Eq. (21), which is supposed to be a finite series containing N terms. The solution is thus complete since all constants have been determined by satisfying the boundary conditions, at N discrete boundary points.

The function coefficients obtained by this method for flow in the three-point-star and four-point-star conduits are listed in Table 3.

The results calculated from these function coefficients are compared with those of Lundgren et al.<sup>[6]</sup> limit case, and it shows very good agreement.

## 2.2 Derivations

From the analytical solutions previously obtained the numerical values of pressure drop-flow rate relation, friction factor-Reynolds Number relation, maximum velocities and mean velocity are evaluated as a function of  $s/r_0$  or  $@$ , the porosity of the array.

### 2.2.1 Pressure Drop-Flow Rate relationship

For volume flow rate Q ,

$$Q = \int_0^{\theta_0} \int_{r_0}^{s/\cos\theta} u r dr d\theta \tag{22}$$

in which  $u$  is given by Eq. (12) for triangular array and Eq. (14) for square array.

For square array, the  $G_j$  in Eq. (14) are related to the tabulated constants  $\delta_j$  (Table 2) by

$$G_j = \delta_j \frac{-(dp/dx)S^2}{4j\mu S^{4j}} \quad (23)$$

For purpose of integration the dimensionless variable

$$\zeta = \frac{r}{r_0} \quad (24)$$

is introduced.

Then substituting Eqs. (14), (23) and (24) into the flow rate integral Eq. (22), one obtains:

$$Q = \left(-\frac{1}{\mu} \frac{dp}{dx}\right) r_0^4 \left\{ \int_0^{\pi/4} \int_1^{s/r_0 \cos \theta} \left[\frac{2}{\pi} \left(\frac{s}{r_0}\right)^2 \ln \zeta - \frac{1}{4} (\zeta^2 - 1) + \sum_{j=1}^4 \frac{\delta_j (r_0/s)^{4j-2}}{4j} \cdot (\zeta^{4j} - \zeta^{-8j}) \cos 4j\theta\right] \zeta d\zeta d\theta \right\} \quad (25)$$

where  $\theta_0 = \frac{\pi}{4}$  has been introduced for the square array.

The integrals appearing in Eq. (25) can be carried out in a straightforward way, giving :

$$Q = \left(-\frac{1}{\mu} \frac{dp}{dx}\right) r_0^4 \text{function} \left(\frac{s}{r_0}\right) \quad (26)$$

where

$$\text{function} \left(\frac{s}{r_0}\right) = \left(\frac{s}{r_0}\right)^4 \cdot \left[\frac{1}{2\pi} (\ln \frac{s}{r_0} + \ln 2 - 3) + \frac{1}{6}\right] + \left(\frac{s}{r_0}\right)^4 \sum_{j=1}^4 \frac{\delta_j}{4j} \cdot \left[\frac{\Lambda_j}{4i+2} + \left(\frac{r_0}{s}\right)^{8j} \frac{\beta_j}{4i-2}\right] + \frac{1}{4} \left(\frac{s}{r_0}\right)^2 - \frac{\pi}{64}$$

where  $\Lambda_j = \int_0^{\pi/4} \frac{\cos 4j\theta}{(\cos \theta)^{4j+2}} d\theta$

$$\beta_j = \int_0^{\pi/4} \frac{\cos 4j\theta}{(\cos \theta)^{2-4j}} d\theta$$

In a similar manner the final result for the flow rate for the triangular array can be obtained :

$$Q = \left(-\frac{1}{\mu} \frac{dp}{dx}\right) r_0^4 \cdot \text{function} \left(\frac{s}{r_0}\right) \quad (27)$$

$$\text{function} \left(\frac{s}{r_0}\right) = \left(\frac{s}{r_0}\right)^4 \cdot \left[\frac{1}{2\pi} (\ln \frac{s}{r_0} - \ln \cos 30^\circ - \frac{3}{2} + \frac{13\sqrt{3}}{216}) + \left(\frac{s}{r_0}\right)^4 \sum_{j=1}^4 \frac{\Delta_j}{6j} \cdot \left[\frac{\Omega_j}{6j+2} + \left(\frac{r_0}{s}\right)^{12j} \frac{x_j}{6j-2}\right] + \frac{\sqrt{3}}{12} \left(\frac{s}{r_0}\right)^2 - \frac{\pi}{96}\right]$$

where  $\Omega_j = \int_0^{\pi/6} \frac{\cos 6j\theta}{(\cos \theta)^{6j+2}} d\theta$ ,  $x_j = \int_0^{\pi/6} \frac{\cos 6j\theta}{(\cos \theta)^{2-6j}} d\theta$

The pressure drop-flow rate relationship as a function of  $s/r_0$  (and of porosity @) is shown on Fig. 4. The porosity is defined as

$$@ = \frac{A_2}{A_1 + A_2} = 1 - \frac{\theta_0}{(s/r_0)^2 \tan \theta_0} \quad (\text{see Fig. 5})$$

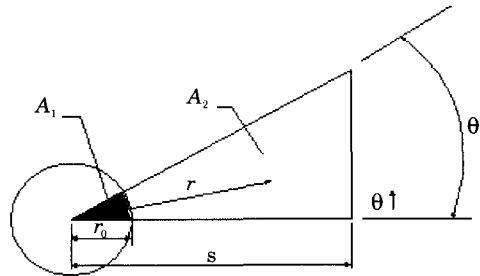


Fig. 4 Geometry Model of Porosity @

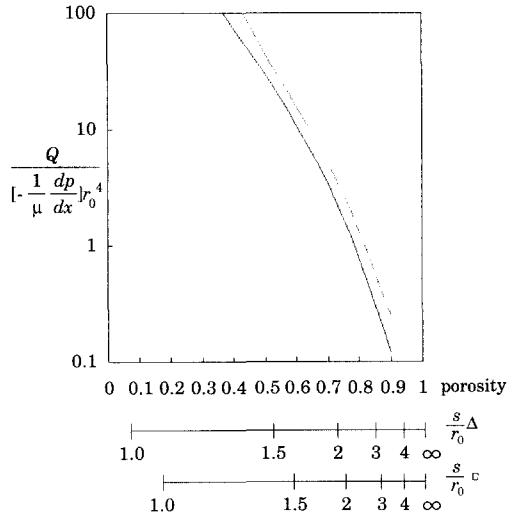


Fig. 5 The Variation of pressure drop - flow rate with porosity and  $\frac{s}{r_0}$

2.2.2 Mean Velocity and Maximum Velocity

Mean velocity can be evaluated from :

$$\bar{u} = \frac{\iint_{A_2} u \, dA}{A_2}$$

in which  $\bar{u}$  is given by Eq. (12), Eq. (14) and Eq. (21) for triangular array, square array and star conduit, respectively. Maximum velocity  $u_0$  for triangular array and square array can be obtained by simply substituting  $(r_0/\cos \frac{\pi}{6}, \frac{\pi}{6})$  and  $(r_0/\cos \frac{\pi}{4}, \frac{\pi}{4})$  into Eq. (12) and Eq. (14) respectively. For star conduit, R=0 should be substituted into Eq. (21) to obtain the maximum velocity. Fig.6 shows the results of dimensionless maximum velocity and mean velocity vs. porosity for triangular and square Array

2.2.3 Friction Factor-Reynolds Number Relationship

Refer to Fig. 4, force balance yields :

$$\tau = \frac{-(dp/dx)A_2}{r_0\theta_0} \tag{28}$$

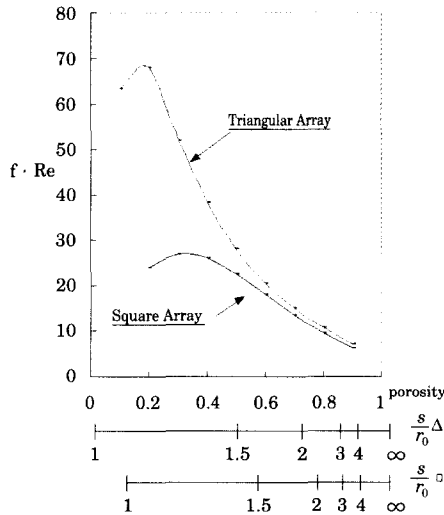


Fig. 6  $f \cdot Re$  vs. porosity and pitch-to-radius ratio  $(\frac{s}{r_0})$

$$\therefore f = \frac{\tau}{\rho \bar{u}^2 / 2} = \frac{-2(dp/dx)A_2}{r_0\theta_0 \rho \bar{u}^2} \tag{29}$$

Let  $Re = \frac{\rho d \bar{u}}{\mu}$   
where  $d = 2r_0$

Eq. (29) yields after rearrangement :

$$f \cdot Re = \left[ \frac{r_0^4}{Q\mu} \left( \frac{-dp}{dx} \right) \right] \left[ \frac{4A_2^2}{\theta_0 r_0^4} \right] \tag{30}$$

The friction factor - Reynolds Number relationship is computed for each array from Eq. (30), and the results are plotted on Fig. 7.

3. GEOMETRIC PARAMETERS FOR A BUNDLE OF RODS

3.1 Analysis

The relationship between the average velocity and shear stress for the flow of any incompressible, time - independent fluid in a channel of arbitrary section is given by

$$\frac{2(\bar{u} - u_w)}{r_h} = \frac{1}{a} \tau_w^{-\xi} \int_{\tau_y}^{\tau_w} \frac{\tau \xi}{\eta} d\tau \tag{31}$$

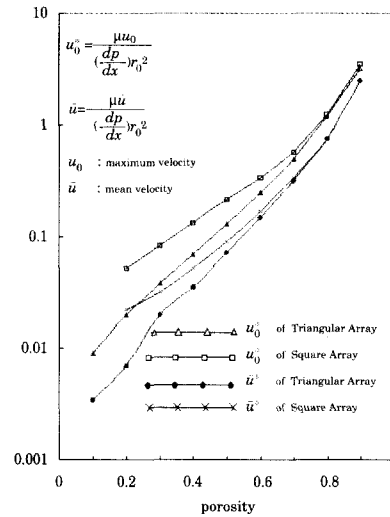


Fig. 7 Dimensionless Maximum Velocity and Mean Velocity vs. Porosity for Triangular and Square Array

the aspect ratio  $\xi$  is equal to  $b/a$ . The constants "a" and "b" are geometric parameters characterizing the shape of the cross section and is nothing to do with the properties of the fluid model.

In Kozicki's paper<sup>[1],[2]</sup>, the general equations for the bulk velocity and maximum velocity have been integrated for a number of different non-Newtonian fluid models and the resulting equations are presented in Kozicki et al.<sup>[1]</sup>.

For Newtonian fluid, Kozicki and Tiu<sup>[1],[2]</sup> presented the equation shown below

$$\frac{2\bar{u}}{r_h} = \frac{1}{a+b} \left( \frac{\tau_w}{\mu} \right) \tag{32}$$

$$\frac{2u_0}{r_h} = \frac{1}{2a} \left( \frac{\tau_w}{\mu} \right) \tag{33}$$

in which it has been assumed that no slip occurs at the boundary of wall.  $r_h$  is called the hydraulic radius and given by

$$r_h = \frac{A}{P}$$

where A is flow cross section area and P is wetted perimeter of the wall boundary

After "a" and "b" are evaluated, return to any different type of non-Newtonian fluid to obtain its maximum velocity, mean velocity, stress-strain rate relationship ....etc.

For instance, for power law fluid, maximum and average velocity can be obtained by using the relations given as follows<sup>[11]</sup>;

$$\frac{2\bar{u}}{r_h} = \left( \frac{\tau_0}{K} \right)^{\frac{1}{n}} \left( \frac{n}{a+bn} \right)$$

$$\frac{2u_0}{r_h} = \left( \frac{\tau_0}{K} \right)^{\frac{1}{n}} \left[ \frac{n}{a(1+n)} \right]$$

with appropriate a and b value from this research.

### 3.2 Calculation of Geometric Parameters

From Eq. (32),

$$a+b = \frac{r_h \bar{\tau}_w}{2\mu \bar{u}} = \frac{A}{P} \frac{1}{2\bar{u}} \frac{1}{\mu} \left[ \frac{A}{P} \left( -\frac{dp}{dx} \right) \right] \tag{34}$$

in which the force balance equation (Eq. (28)) has been substituted for  $\bar{\tau}_w$ .

For the case of a unit element between the cylinders (see Fig. 2),

$$A = \int_0^{\pi/6} \int_{r_0}^{s/\cos\theta} r \, dr \, d\theta = \frac{1}{2} r_0^2 \left[ \left( \frac{s}{r_0} \right)^2 - \frac{\pi}{6} \right] \tag{35}$$

: triangular array

$$A = \int_0^{\pi/6} \int_{r_0}^{s/\cos\theta} r \, dr \, d\theta = \frac{1}{2} r_0^2 \left[ \left( \frac{s}{r_0} \right)^2 - \frac{\pi}{4} \right]$$

: square array

where  $P = r_0 \theta_0$ ,  $\theta_0 = \frac{\pi}{6}$  : triangular array

$\theta_0 = \frac{\pi}{4}$  : square array

Besides, the values of  $u_0$  have been obtained previously, so that the numerical values of (a+b) can be calculated. From Eq. (32) and (33),

$$2 \left( \frac{u_0}{\bar{u}} \right) - 1 = \frac{b}{a} \tag{35}$$

From Eq. (35), the numerical values of (b/a) can be easily evaluated from the values of  $u_0$  and  $\bar{u}$  previously obtained.

Finally, Eq. (34) and Eq. (35) are solved simultaneously for a and b. The obtained values of a and b are plotted as a function of porosity and as a function of  $s/r_0$  on Fig. 8.

## 4. RESULTS AND DISCUSSION

The present numerical calculations generalized the Mooney-Rabinowitsch equation to handle various non-circular geometries. Eq. (20) was written in terms of two geometric



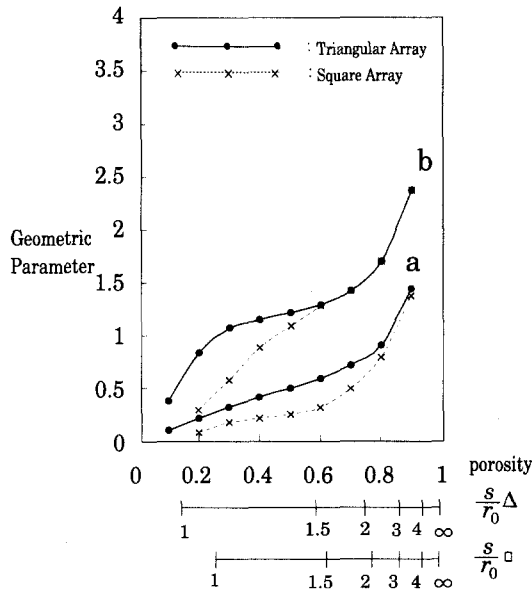


Fig. 8 Geometric Parameter ( a and b ) vs. Porosity and  $\frac{s}{r_0}$

constants "a" and "b", then suggested a generalization by defining an averaged wall shear stress for any shape of cross section. This amounted to assuming the simple shear law applied to arbitrary shear fields. All that is required to calculate the values of "a" and "b" from the solution for the same duct in laminar fully developed Newtonian flow which has been completely surveyed by Shah and London<sup>[10]</sup>, and is now readily available. Values and expressions for the estimation of geometric parameters a and b, determined for the different cross sectional shape of the duct. For circular ducts a=0.25, b=0.75, and for parallel plate ducts a=0.5, b=1.0. Irvine et al.<sup>[18]</sup> extended the calculation a and b to eccentric annular, rhombic ducts and even isosceles triangular open channels. Tung<sup>[19]</sup> presented a limited experimental verification of Kozicki's method for the flow of a power law fluid in an isosceles triangular duct with an apex angle of 11.5 degrees. Chang<sup>[20]</sup> made a systematic experimental

study of the flow of power law fluid in an isosceles triangular duct with an apex angle of 10 degrees. It was felt that such extreme geometry with its widely varying values of local wall shear stress around circumference would show the Kozicki's assumptions completely good for the comparison. Table 4 lists values of additional geometric parameters for a large number of different duct cross sections<sup>[18]</sup>.

The present numerical results of geometric parameters a and b for both triangular and square arrays are listed on Table 5. It is easily seen either from Fig. 8 or from Table 5 that a and b become the same as the porosity gets large. This is as expected, since at large spacings, where there is little effect of neighboring rods, the flow passages of the two arrays are almost geometrically similar.

Finally, an example is given to illustrate how the results are used. The dimensionless velocity for a power law fluid for which  $f(\tau)=(\tau/k)^{1/n}$  will be evaluated.

Example : Evaluate the dimensionless mean velocity for a steady state laminar power law fluid between cylinders arranged in triangular arrays of  $s/r_0 = 1.1$ ,  $s/r_0 = 1$ .

The mean velocity expression for power law flow is given to be

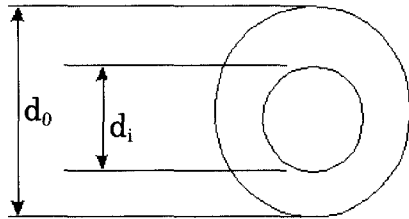
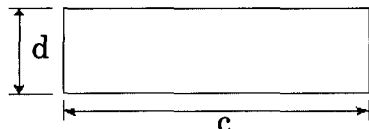
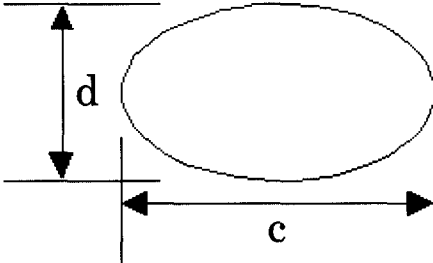

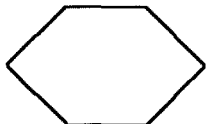
$$\frac{2\bar{u}}{r_h} = \left(\frac{\tau_w}{K}\right)^{1/n} \left(\frac{n}{a+bn}\right) \tag{a}$$

in which

$$r_h = \frac{A}{P} = \frac{\frac{1}{2} r_0^2 \left[ \frac{1}{\sqrt{3}} \left(\frac{s}{r_0}\right)^2 - \frac{\pi}{6} \right]}{r_0 \frac{\pi}{6}} = \frac{3r_0 \left[ \frac{1}{\sqrt{3}} \left(\frac{s}{r_0}\right)^2 - \frac{\pi}{6} \right]}{\pi}$$

also,

**Table 4. Geometric Parameters for Duct Flows<sup>(18)</sup>a**

| Geometry  | $\alpha^*$       | a      | b      |
|---|------------------|--------|--------|
|  <p>Concentric annuli</p> <p><math>\alpha^* = \frac{d_i}{d_0}</math></p> | 0.1              | 0.0445 | 0.9510 |
|   | 0.2              | 0.4693 | 0.9739 |
|   | 0.3              | 0.4817 | 0.9847 |
|   | 0.4              | 0.4890 | 0.9911 |
|   | 0.5              | 0.4935 | 0.9946 |
|   | 0.6              | 0.4965 | 0.9972 |
|   | 0.7              | 0.4983 | 0.9987 |
|   | 0.8              | 0.4992 | 0.9994 |
|   | 0.9              | 0.4997 | 1.0000 |
|   | 1.0 <sup>b</sup> | 0.5000 | 1.0000 |
|  <p>Rectangular</p> <p><math>\alpha^* = \frac{c}{d}</math></p>           | 0.0              | 0.5000 | 1.0000 |
|   | 0.25             | 0.3212 | 0.8482 |
|   | 0.50             | 0.2440 | 0.7276 |
|   | 0.75             | 0.2178 | 0.6866 |
|   | 1.00             | 0.2121 | 0.6772 |
|  <p>Elliptical</p> <p><math>\alpha^* = \frac{c}{d}</math></p>           | 0.00             | 0.3084 | 0.9253 |
|   | 0.10             | 0.3018 | 0.9053 |
|   | 0.20             | 0.2907 | 0.8720 |
|   | 0.30             | 0.2796 | 0.8389 |
|   | 0.40             | 0.2702 | 0.8107 |
|   | 0.50             | 0.2629 | 0.7886 |
|   | 0.60             | 0.2575 | 0.7725 |
|   | 0.70             | 0.2538 | 0.7614 |
|   | 0.80             | 0.2515 | 0.7546 |
|   | 0.90             | 0.2504 | 0.7510 |
| 1.00 <sup>c</sup>   | 0.2500           | 0.7500 |        |
|  <p>Isosceles triangular</p> <p><math>2\phi</math></p>                 | $2\phi$ (deg)    |        |        |
|   | 10               | 0.1547 | 0.6278 |
|   | 20               | 0.1693 | 0.6332 |
|   | 40               | 0.1840 | 0.6422 |
|   | 60               | 0.1875 | 0.6462 |
|   | 80               | 0.1849 | 0.6438 |
|   | 90               | 0.1830 | 0.6395 |
|  <p>Regular polygon (N sides)</p>                                      | $\frac{N}{4}$    | 0.2121 | 0.6771 |
|   | 5                | 0.2245 | 0.6966 |
|   | 6                | 0.2316 | 0.7092 |
|   | 8                | 0.2391 | 0.7241 |

a Data from<sup>(18)</sup>

b Parallel plates

c Circle

**Table 5. Numerical Values of Geometric Parameters**

| Triangular |      |      | Square  |      |      |
|------------|------|------|---------|------|------|
| $s/r_0$    | a    | b    | $s/r_0$ | a    | b    |
| 4.00       | 1.98 | 3.00 | 4.00    | 2.02 | 3.34 |
| 2.00       | 0.86 | 1.59 | 2.00    | 0.79 | 1.73 |
| 1.50       | 0.61 | 1.33 | 1.50    | 0.49 | 1.36 |
| 1.20       | 0.39 | 1.17 | 1.20    | 0.25 | 1.01 |
| 1.10       | 0.27 | 1.00 | 1.10    | 0.18 | 0.74 |
| 1.05       | 0.18 | 0.78 | 1.05    | 0.13 | 0.55 |
| 1.04       | 0.16 | 0.71 | 1.00    | 0.09 | 0.32 |
| 1.03       | 0.14 | 0.62 |         |      |      |
| 1.02       | 0.12 | 0.53 |         |      |      |
| 1.01       | 0.10 | 0.43 |         |      |      |
| 1.00       | 0.08 | 0.31 |         |      |      |

$$\tau_w = \left(-\frac{dp}{dx} \cdot \frac{A}{P}\right) = \left(-\frac{dp}{dx} \cdot r_h\right)$$

Substituting this into Eq. (a),

$$\frac{2\bar{u}}{r_h} \frac{1}{\left(-\frac{1}{K} \frac{dp}{dx}\right)^{\frac{1}{n}} r_h^{\frac{1}{n}}} = \frac{n}{a+bn}$$

$$\frac{2\bar{u}}{\left(-\frac{1}{K} \frac{dp}{dx}\right)^{\frac{1}{n}} (r_0)^{\frac{1}{n+1}}} = \frac{n}{a+bn} \left\{ \frac{3}{\pi} \left[ \frac{1}{3} \left(\frac{s}{r_0}\right)^2 - \frac{\pi}{6} \right] \right\}^{\frac{1}{n+1}} \quad (b)$$

The term on the left hand side of Eq. (b) is defined as the dimensionless mean velocity and can be easily obtained as follows :

(1) assume  $n = 0.5$

for  $s/r_0=1.1$  :  $a = 0.27$   
 $b = 1.00$

substituting into the right hand side of Eq. (b),

$$\frac{2\bar{u}}{\left(-\frac{1}{K} \frac{dp}{dx}\right)^{\frac{1}{n}} (r_0)^{\frac{1}{n+1}}} = 0.003$$

for  $s/r_0=1$  :  $a = 0.08$   
 $b = 0.31$

Substituting the values of  $n, s/r_0, a$  and  $b$  into the right hand side of Eq. (b) gives :

$$\frac{2\bar{u}}{\left(-\frac{1}{K} \frac{dp}{dx}\right)^{\frac{1}{n}} (r_0)^{\frac{1}{n+1}}} = 0.0003$$

(2) assume  $n = 0.8$

for  $s/r_0=1.1$  :  $a = 0.27$   
 $b = 1.00$

Substituting the values of  $n, s/r_0, a$  and  $b$  into Eq. (b),

$$\frac{2\bar{u}}{\left(-\frac{1}{K} \frac{dp}{dx}\right)^{\frac{1}{n}} (r_0)^{\frac{1}{n+1}}} = 0.013$$

for  $s/r_0=1$  :  $a = 0.08$   
 $b = 0.31$

Again from Eq. (b),

$$\frac{2\bar{u}}{\left(-\frac{1}{K} \frac{dp}{dx}\right)^{\frac{1}{n}} (r_0)^{\frac{1}{n+1}}} = 0.003$$

### 5. CONCLUSION

Considerable interest has evolved in the flow of non-Newtonian fluids in channels of noncircular cross section in compact heat exchangers. Analytical solution was developed for prediction of the flow rate and maximum velocity in steady laminar flow of any incompressible, time-independent non-Newtonian fluids in straight closed and open channels of arbitrary, but axially unchanging cross section. The geometric parameters and function of shear stress describing the behavior of the fluid model were evaluated for flow between a bundle of rods arranged in triangular and square arrays for which the necessary data was available. Examples have been given to illustrate the usefulness and applicability of the present analytical method. The present method can be utilized equally to the complex flow situations such as arbitrarily cross-sectional flow geometry. The geometric parameters may be calculated in such situations from the simple power law fluid type.

The general flow rate equation was integrated to show the utility of the general result and to present relationships for a plenty of fluids of interest to engineers. The product of Fanning friction factor and Reynolds number were also estimated in order to apply to the flow situations of the present interest such as channels arranged in triangular and square arrays as well as to time-independent non-Newtonian fluids. A single equation is valid enough to consider the relationship existing in the laminar flow region between the Fanning friction factor and the new generalized Reynolds number,  $Re^*$ ,  $f=16/Re^*$ . Numerical values of dimensionless maximum velocities, mean velocities, pressure-drop-flow parameters and friction factors were evaluated as a function of porosity and pitch-to-radius ratio. Conclusively, the methods applied make it possible to characterize and represent quantitatively the geometry of the flow situation in evaluations of the pressure gradient and mean velocity or maximum velocity

#### NOMENCLATURE

|           |                                   |
|-----------|-----------------------------------|
| $A$       | : flow cross-sectional area       |
| $a$       | : geometric parameter             |
| $b$       | : geometric parameter             |
| $d$       | : diameter of rod                 |
| $P$       | : wetted perimeter                |
| $Q$       | : volume flow rate                |
| $r$       | : radius                          |
| $r_0$     | : radius of rod                   |
| $r_h$     | : hydraulic radius                |
| $K$       | : fluid index for power law fluid |
| $s$       | : half pitch of rod array         |
| $u$       | : axial velocity                  |
| $u_0$     | : axial maximum velocity          |
| $\bar{u}$ | : axial mean velocity             |

|                |                                 |
|----------------|---------------------------------|
| $x$            | : axial position                |
| @              | : porosity                      |
| $\rho$         | : density of fluid              |
| $\mu$          | : absolute viscosity            |
| $\eta$         | : non-Newtonian viscosity       |
| $\tau$         | : shear stress                  |
| $\bar{\tau}_w$ | : mean shear stress at the wall |
| $\tau_y$       | : yield stress                  |

#### REFERENCE

1. W. Kozicki, C.H. Chou, and C. Tiu, "Non-Newtonian Flow in Ducts of Arbitrary Cross-Sectional Shape", Chem. Eng. Sci., vol. 21, pp.665, 1966.
2. W. Kozicki, and C. Tiu, "Non-Newtonian Flow through Open Channels", Can. J. Chem. Eng., vol. 45, pp.127, 1967.
3. W. Kozicki and C. Tiu, "Improved Parametric Characterization of Flow Geometries", Can. J. Chem. Eng., vol. 49, pp. 562, 1971.
4. C. Tiu, W. Kozicki, and T. Q. Phung, "Improved Parameters for Some Flows Channels", Can. J. Chem. Eng., vol. 46, pp.389-393, 1968.
5. C. Tiu and W. Kozicki, "Geometric Parameters for Open Circular Channels", Can. J. Chem. Eng., Vol. 47. pp.438-439, 1969.
6. A. B .Metzner and J. C Reed, "Flow of Non-Correction of the Laminar, Transition, and Turbulent Flow Regions", AIChE J., vol. 1, pp.434, 1955.
7. R. B. Bird, W. E .Stewart, and E .N. Lightfoot, Transport Phenomena, John Wiley, New York,1960.
8. T. S. Lundgren, E. M. Sparrow, and J. B. Starr, "Pressure Drops Due to the Entrance Region in Ducts of Arbitrary Cross Sections", Trans. of ASME, 86D, pp.622, 1964
9. F. S. Shih, "Laminar Flow axisymmetric conduits by a rational approach", Can. J. Chem. Eng., vol. 45, pp.285, 1967.
10. R. K. Shah and A. L. London, Laminar Flow Forced Convection in Ducts, Supplement 1 to Advances in Heat Transfer (T. F. Irvine, Jr. And

- J. P. Hartnett ed. ), Academic Press, New York, 1978.
11. J. P. Hartnett and M. Kostic, Heat Transfer to Newtonian and Non-Newtonian Fluids in Rectangular Ducts, Advances in Heat Transfer (T. F. Irvine, Jr. And J. P. Hartnett ed.), 19, Academic Press, New York, 1989.
  12. V. S. Arpaci and P. S. Larsen, Conduction Heat Transfer, Addison-Wesley Publishing Co, Inc, Reading, Massachusetts, 1996.
  13. S. Kakac and Y. Yener, Heat Conduction, Hemisphere Publishing Corporation, New York, 1985.
  14. G. E. Myers, Analytical Methods in Conduction Heat Transfer, Genium Publishing Corporation, New York, 1987.
  15. F. B. Hildebrand, Advanced Calculus for Applications, 2nd ed, prentice-Hall, Inc. Englewood Cliffs, New Jersey, 1976.
  16. W. M. Kays and M. Crawford, Convective Heat and Mass Transfer, McGraw-Hill Book Inc, New York, 1980.
  17. F. M. White, Viscous Fluid Flow, McGraw-Hill Inc, New York, 1974.
  18. T. F. Irvine, Jr. and J. Karni, Non-Newtonian Fluid Flow and Heat Transfer, Handbook of Single Phase Convective Heat Transfer, S. Kakac, R. K. Shah, and W. Aung ed.), Wiley, New York, 1987.
  19. S. S. Tung, Experimental Study of Non-Newtonian Flow in a Narrow Isosceles Triangular Duct, Ph.D. Thesis, Mechanical Engineering Department , State University of New York at Stony Brook, Stony Brook, New York, 1977.
  20. T. D. Chang, Fully Developed Power Law Fluid Pressure Drops in a Narrow Isosceles Triangular Duct. M. S. Thesis, Mechanical Engineering Department, State University of New York at Stony Brook, Stony Brook, New York, 1981.

## 저 자 소 개



### 이동렬(李東烈)

63년생. 1986년 연세대학교 기계공학과 졸업. 1989년 Oklahoma state University 기계공학과 졸업(석사). 1995년 State University of New York at Stony Brook 기계공학과 졸업(박사). 1995년~1996년 State University of New York at Stony Brook, Thermal Science Research Laboratory. 1996년~1997년 삼성자동차(주)기술연구소. 1997년~현재 대구가톨릭대학교 기계자동차공학부 조교수